Direct State-Space Model for Model Predictive Control of Multi-Level Power Converters

Samuel Jupin, Ionel Vechiu, Gerardo Tapia

Direct State-Space Model for Model Predictive Control of Multi-Level Power Converters

Samuel JUPIN; Ionel VECHIU
ESTIA-RECHERCHE
ESTIA
Bidart, FRANCE

Gerardo TAPIA
Faculty of Engineering, Gipuzkoa
University of the Basque Country, UPV/EHU
San Sebastián, SPAIN

***Abstract*— With reliability and flexibility criteria surging, multi-level converters become of growing interest for high-power medium-voltage renewable energy applications. Specific objectives are met with specialized intelligent controls. The goal of this paper is to present a universal intelligent controller able to manage all degrees of freedom of multi-level power converters and any paradigm. To do so, a couple formed by a model and an appropriate optimizer is introduced, relying on state-space representation and Dijkstra algorithm. The obtained controller does not require modulation and could control any topology on any application under any constraints. In order to demonstrate the effectiveness of this controller, the operation of two multi-level converter topologies is investigated in simulation.**

Keywords—MPC; multi-level power converters; direct power control; neutral point clamped; flying capacitor; Dijsktra algorithm; branch and bound

I. INTRODUCTION

Renewable energies are foreseen to become the main sources of electricity in the future [1], and are already being massively implemented. However, they entail weakness and further unpredictability in the grid, requiring a reinforcement of the grid actuators: power converters. Because of renewable energies geographical distribution, the grid voltage and frequency become sensitive to the various power injections and consumptions. These flows are more and more managed by the power converters, especially multi-level ones in the case of grid applications, as they support higher levels of power, decrease the Total Harmonic Distortion (THD), have a better efficiency and offer further freedom than their simpler counterparts. In fact, heightened power requirements, reliability issues and energy quality specifications also call for more intelligence in power converters [2]. Various control strategies are currently being developed, such as Model Predictive Control (MPC) [3] or Sliding-Mode Control [4][5]. MPC employs optimization to supply intelligence and robustness [6]. However, it needs a coherent model and a systematic optimizer. Usual models for multi-level power converters (ML-PCs) are based on a modulation, which changes with every demand and specification, therefore limiting the overall intelligence of the control. In order to preserve MPC's capability, it is interesting to occult this modulation aspect and to directly generate the commutation orders of each IGBT. Consequently, in this paper, a general direct modelling methodology is presented along with a MPC algorithm solving the specific hurdles the absence of modulation imposes. The model obtained can be extended to any multi-level power converter application, while the proposed controller generates optimal control for any problem under the form of this model. Therefore, the developed methodology can be extended to a large variety of topologies and applications and can thus be considered general or universal. This paper focuses on using the proposed controller based on MPC relying on state-space representation and Dijkstra optimization with two multi-level converter topologies: Neutral Point Clamped (NPC) and Flying Capacitor (FC) — Fig.1.

II. STATE-SPACE REPRESENTATION FOR MULTI-LEVEL POWER CONVERTERS

A. Methodology

To reach the objective described hereafter, it is impossible to express the model of ML-PCs with the usual linear state-space representation as in (1), because of the strong non-linearity between the switching commands and the electrical variables. However, each binding position of the converter leads to a set of equations described by Kirchhoff Current (KCL) and Voltage laws (KVL). These sets of equations can be combined by applying the theorem of superposition, therefore supplying a state-space model for ML-PCs. Mathematically, this model is shown in (2):

$$\mathbf{x}(k+1) = \mathbf{A}\mathbf{x}(k) + \mathbf{B}\mathbf{u}(k) + \mathbf{E}\mathbf{d}(k) \quad (1)$$

$$\mathbf{x}(k+1) = \mathbf{A}(\mathbf{u}(k))\mathbf{x}(k) + \mathbf{B}\mathbf{d}(k), \quad (2)$$

where **x** is the state vector, containing all accumulative variables, e.g. capacitors' voltages, and **d** the disturbance vector, composed of all uncontrolled inputs, such as grid voltages. The switching states, i.e. the control input **u**(*k*), appear in the **A** matrix. This signal is not continuous, as there is only a limited number of switching states. This number, related to the topology and to the number of levels of the power converter considered, defines the cardinal of the control set. For example, a Three-Level Neutral Point Clamped (3L-NPC) entices 27 different switching states, when a Three-Level Flying Capacitor (3L-FC) does 64 and a Five-Level Neutral Point Clamped (5L-NPC) topology presents 125.

B. Remarkable Properties

The notion of quantified control is extended to the **A** matrix: instead of a single control-dependent matrix, it becomes a set of matrices, each related to one switching order. Though unusual,

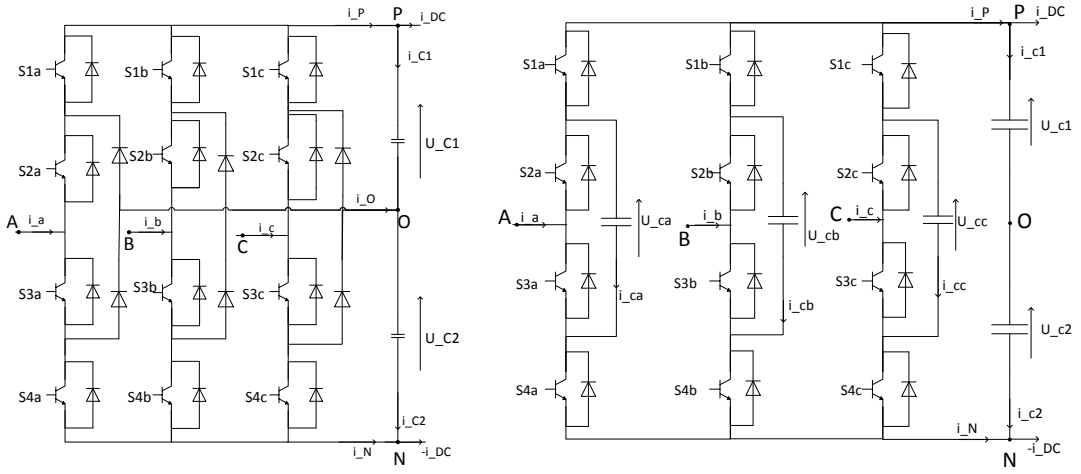

(a) (b)

Fig. 1: Investigated topologies (a) Neutral Point Clamped. (b) Flying Capacitor

this expression shares similitude with parameter-dependent models and continuous-by-piece representations: as long as the control does not change, the previous model accurately and linearly depicts the dynamics of the system. Eventually, this system is linear by piece, leading to low-cost prediction computing.

The general form of the model also encompasses usual state-space representations, allowing to extend it to incorporate any power conversion application: different topologies, different types of sources, of grids and of filters can all be defined through the previous model. For a given application, the ascending diagonal blocks of **A** change according to the topology while for a given topology, its descending diagonal blocks vary according to the connected dynamics as shown in (3).

$$\mathbf{A} = \begin{bmatrix} \mathbf{A_{AC}} & \mathbf{A_{conv\_1}} \\ \mathbf{A_{conv\_2}} & \mathbf{A_{DC}} \end{bmatrix} \tag{3}$$

The universality of this model allows a MPC controller employing this canonical model to be adapted to any multi-level power converter application.

III. Generic Model Predictive Control Algorithm for Power Converters

A. ML-PC Requirements and Impediments

ML-PC specifications can be characterized in three categories. First, the quality of the conversion, described by the wave quality, the active and reactive powers transferred, absorbed or generated by the system, as well as the DC-link voltage. Secondly, the internal considerations, illustrated with the FC topology and its constitutive capacitors. Finally, reliability and efficiency considerations: the distribution of the energy among the switching devices, the overall losses and the switching frequency all contribute to the global health and performance of the converter. This last category is symptomatic of the maturation of ML-PC technology and entails complications in the control strategies developed in the previous generations [7]. Indeed, in order to adapt to these new expectations, modulation strategies gain in complexity and specialization, therefore confining their interest. For instance, modulations can be designed specifically to address one or the other of the previously mentioned requirements, but attempting to tackle them all becomes tremendously difficult as the reliability criteria keep stacking. The objective of direct control MPC is to bypass this modulation block and to straightforwardly generate the switching orders taking into account any of all these issues.

MPC relies on two functions: prediction and optimization [5]. It combines a discrete state-space model and an optimization algorithm to deduce an optimal control sequence, then applied to the current step. This closed-loop optimization is both the main flaw and the greatest strength of MPC, as it is extremely powerful and computationally heavy. This matter is amplified by the high frequency required when directly controlling the switching orders. Such a high frequency means that all computations have to be performed in only a few microseconds, regular MPC requiring to issue a command in a fraction of the sample period to perform. The progress of industrial informatics offers a perspective to implement relatively heavy computations in a short time of several hundreds of microseconds, i.e. a frequency between 1 and 10 kHz.

As seen previously, the model of ML-PCs is non-linear with respect to the control. It is also based on a finite control-set, as there is a limited number of switching possibilities. These two constraints disqualify the usual MPC frame, built around Linear Quadratic Optimization, hence around a continuous control-set. In fact, this framework also imposes strict limitations on the objectives and considerations expressed in the cost function. Reliability requirements in particular can be tough to convey. Eventually, it appears necessary to develop a different approach to implement MPC on ML-PCs. Miscellaneous propositions have already been made in the past years, with different optimization problems and solutions [3].

B. Finite Control-Set MPC

The very first step to adapt MPC to ML-PC is to free up computational time. Finite Control-Set MPC can be used to perform this first step (Fig. 2). This algorithm focuses on staying one step ahead of the system, thus releasing computational time:

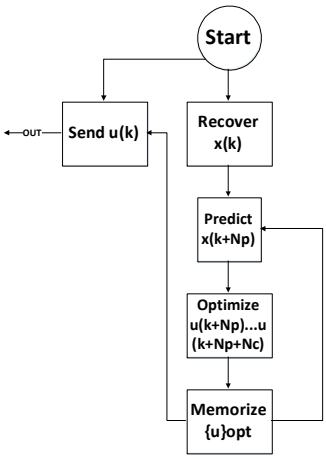

Fig. 2: Finite Control Set MPC algorithm

when called, it first supplies the previously computed optimal control, then applies a prediction previous to the optimization. This means that, for an instant k, the controller is not computing the optimal control $\{\mathbf{u}(k), \dots, \mathbf{u}(k+N_c)\}$, but $\{\mathbf{u}(k+N_p), \dots, \mathbf{u}(k+N_p+N_c)\}$, with N_p and N_c being respectively the horizons of prediction and control. It is equivalent to planning the next step while still in mid-air. With this strategy, all the time between two sample instants can be exploited to run the optimization algorithm, enabling direct control of power converters. This algorithm has been used to perform MPC for unitary horizons [8], but the exponential nature of the optimization problem made it impossible to extend it to any wider horizon.

C. Application of Graph Theory

1) Tree Definition

From the model aforementioned, sample instants can be designated by state-vectors **x**. From a given state-vector **x**(k), depending on the control input applied, a fixed number of other state-vectors **x**(k+1) is accessible. This is made possible by the quantified control set. Defining a cost function representing the distance to various control objectives, it leads to a tree vision: nodes are state-vectors and arcs weigh according to a cost function Γ. At this point, the nature of this function is free. Any mathematical expression can be considered, with a special care on complexity, as heavy computations are to be avoided. Thus, the tree obtained is shown in Fig. 3.

2) Path-Searching Algorithms

From this base, the most intuitive way to present the optimization problem is by a shortest path search. Indeed, the optimal control is the route minimizing the total cost from the source node, being the given initial state, to a destination node, defined by the number of actual sample periods needed to reach it. This number is the control horizon, N_c. The optimization problem is expressed through a cost function, whose design does not necessitate linearity, but whose use requires computational simplicity. Several algorithms perform shortest-path search [9]. Amongst them, Brute Force, Greed, Bellman, and Dijkstra Algorithms [10] were considered. Because it guarantees finding the optimal solution, contrarily to greedy algorithms, and is polynomial, contrarily to brute force, the Dijkstra algorithm is preferred. This solution builds a set of considered paths,

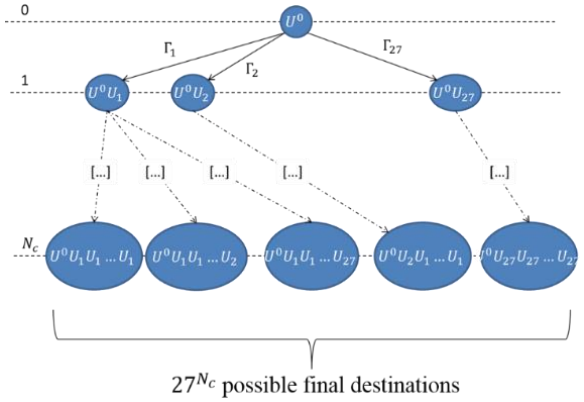

Fig. 3: Tree of possibilities for 3L-NPC

extending it until reaching the desired node by following the protocol presented in Fig. 4.

In order to diminish computational costs, tracking errors are considered with the Manhattan norm (4) rather than the usual quadratic norm.

$$d(\mathbf{y_{ref}}, \mathbf{y}) = |\mathbf{y_{ref}} - \mathbf{y}| \tag{4}$$

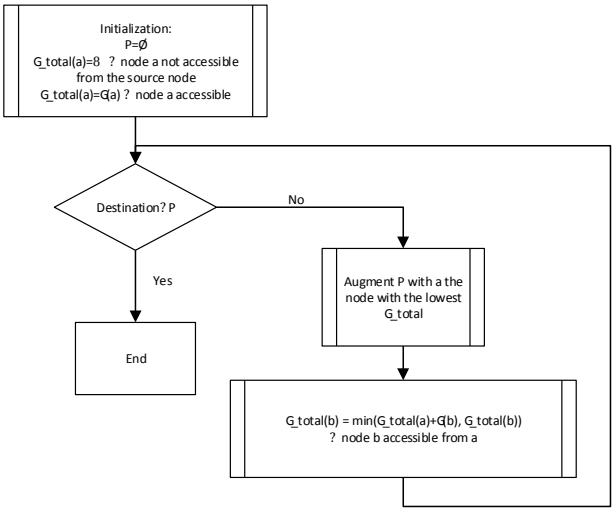

Fig. 4: Dijkstra algorithm

IV. Study on Grid-Connected Converters

A. Context Overview

In order to prove the effectiveness and the interest of the control design previously introduced, simulations are run on general applications. Two case studies are presented considering a power converter used to bind voltage-setting components (Fig. 5). A RL-filter lies between the AC-side and the power converter. The corresponding submatrix $\mathbf{A_{AC}}$ is presented in (5). So far, the DC source/load is considered inertia-less, as shown in (6).

$$\mathbf{A_{AC}} = -\frac{R_g}{L_g}\mathbf{I_3} \tag{5}$$

$$\mathbf{A_{DC}} = \mathbf{0_2} \tag{6}$$

In the first case study, the most widespread topology, Neutral Point Clamped, is investigated. The second case study is devoted to another promising topology for unpredictable power intakes: the Flying Capacitor. By construction, these two topologies do not have exactly the same requirements. However, for the investigated case study, they are both used as rectifiers and share common objectives: tracking of the active and reactive power set-points, P_{ref} and Q_{ref}, as well as the balance between the two capacitor voltages $\Delta u_{ref} = (U_{\_c1} - U_{\_c2})_{ref}$. Traditional control manages these various objectives with a double control-loop (inner fast current-loop, outer slower voltage-loop) and a modulation strategy. Consequently, two controllers have to be adjusted and the modulation strategy has to be designed to consider other demands, such as harmonic elimination or energy distribution. The objective of the simulations is to check that the developed MPC controller manages these three tracking instructions and generates the switching signals. The following results are all obtained with a sample period of 200 µs and a total horizon of 3: the prediction horizon is of one period and the control horizon of two. The physical parameters are presented in Table 1.

TABLE 1: SIMULATION PARAMETERS

Parameter	R_g (Ω)	L_g (H)	C (mF)	U_{grid} (V)	f_{grid} (Hz)	U_{DC} (V)
Value	10	0.03	3.3	230	50	700

B. Neutral Point Clamped

This topology is cheap and reliable, well-known and documented. It is used in a large variety of fields, from industrial machinery to train traction [11], [12]. The scheme displayed in Fig. 1(a) points out that each phase can be hooked up three ways: to V_P, V_0 or V_N. The notation $S_{xi} = 1$ indicates that the phase x is bound to the point i (i = 0 for O, 1 for P, and 2 for N), as shown in Table 2. The previous methodology leads to the set (7) to (12), from which the matrices $\mathbf{A_{conv\_1}}$, $\mathbf{A_{conv\_2}}$ and $\mathbf{B}$ are derived as displayed in (13), (14) and (15), with $\mathbf{x}^T=[i_a\ i_b\ i_c\ U_{c1}\ U_{c2}]$ and $\mathbf{d}^T=[V_{ga}\ V_{gb}\ V_{gc}\ i_{DC}]$. After discretization, this model is implemented in the optimization algorithm, with a cost function containing the previously described objectives.

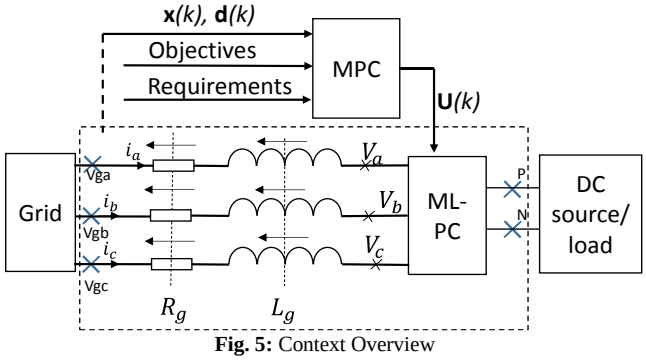

Fig. 5: Context Overview

The reactive and active powers are derived from the state thanks to the Concordia transform.

$$i_{c1} = C dU_{c1}/dt = i_p - i_{DC} \quad (7)$$

$$i_{c2} = C dU_{c2}/dt = -i_{DC} - i_n \quad (8)$$

$$V_{gx} - V_0 = R_g i_x + L_g di_x/dt + S_{x1}U_{c1} - S_{x2}U_{c2} \quad (9)$$

$$i_p = S_{a1}i_a + S_{b1}i_b + S_{c1}i_c \quad (10)$$

$$i_n = S_{a2}i_a + S_{b2}i_b + S_{c2}i_c \quad (11)$$

$$V_0 = 0 \quad (12)$$

$$\mathbf{A^T_{conv\_1}} = \frac{1}{L_g}\begin{bmatrix} -S_{a1} & -S_{b1} & -S_{c1} \\ S_{a2} & S_{b2} & S_{c2} \end{bmatrix} \quad (13)$$

$$\mathbf{A_{conv\_2}} = \frac{1}{C}\begin{bmatrix} S_{a1} & S_{b1} & S_{c1} \\ -S_{a2} & -S_{b2} & -S_{c2} \end{bmatrix} \quad (14)$$

$$\mathbf{B} = \frac{1}{L_g C}\begin{bmatrix} \mathbf{I_3}C & \mathbf{O_{3,1}} \\ \mathbf{O_{1,3}} & L_g \\ \mathbf{O_{1,3}} & L_g \end{bmatrix} \quad (15)$$

TABLE 2: SWITCHING STATES OF 3L-NPC

Control Variable	S_{1x}	S_{2x}	S_{3x}	S_{4x}	Point of connection
S_{x0}	0	1	1	0	O
S_{x1}	1	1	0	0	P
S_{x2}	0	0	1	1	N

The simulation results prove the ability of the controller to manage the aforementioned objectives and to generate direct switching orders. It considers various losses to be minimized, as shown in Figs. 6 to 9. Indeed, the simulation results presented in Figs. 6 and 7 have been obtained with a low consideration on the number of commutations, leading to higher switching frequency, while Figs. 8 and 9 show the results obtained when the objective is to limit the switching frequency. The results show that the controller manages to generate different switching orders to adapt to new considerations. However, advances in performance or savings induce decline in the opposite category. The cost function used in the depicted simulations focuses more on active power tracking than on reactive power tracking, hence the observed fluctuations. On an i5 processor with 2.3 GHz frequency, solving the optimisation problem takes a mean time of 10µs.

TABLE 3: SWITCHING STATES OF 3L-FC

Control Variable	S_{1x}	S_{2x}	S_{3x}	S_{4x}	Point of connection
S_{x0-}	0	1	0	1	N by C
S_{x1}	1	1	0	0	P
S_{x0+}	1	0	1	0	P by C
S_{x2}	0	0	1	1	N

C. Flying Capacitor

Hindered by its additional price and major difficulties to control its inner capacitors, the FC topology still presents interesting features, especially for grid applications, as those inner capacitors serve as a buffer, offering a certain inertia to the converter. Theoretically, this topology is the most adapted to smart grids and renewable energy integration [12].

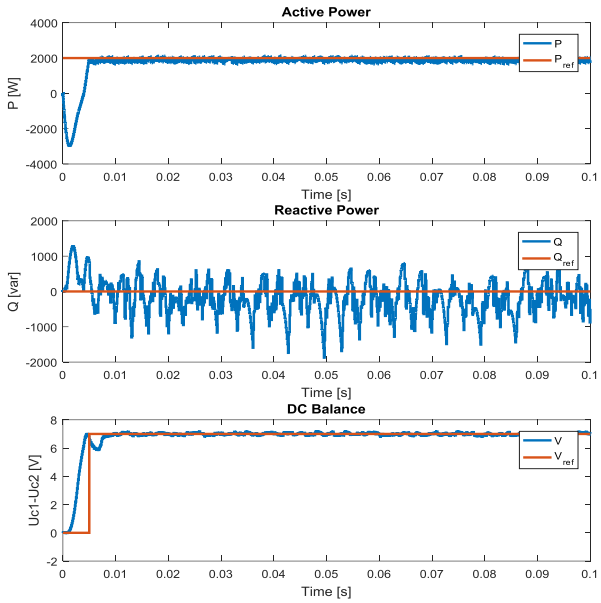

Fig. 6: 3L-NPC tracking, low consideration for the switching frequency

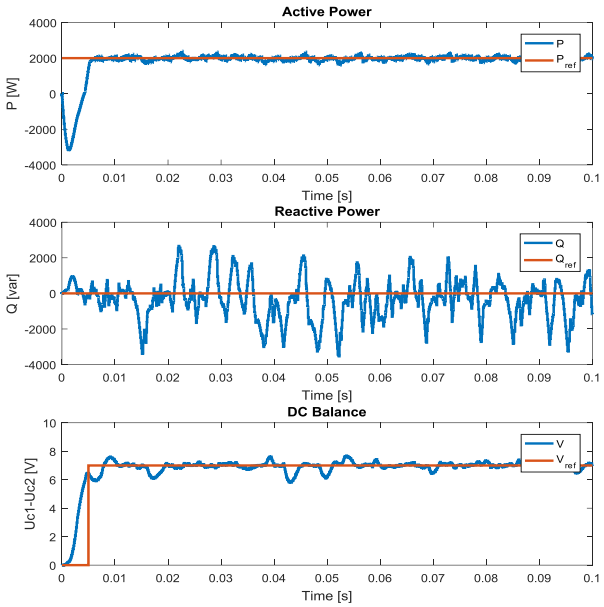

Fig. 7: 3L-NPC tracking, high consideration for the switching frequency

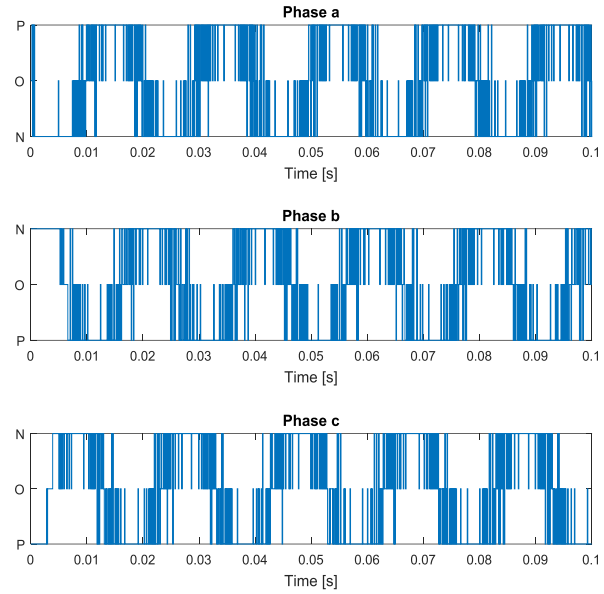

Fig. 8: 3L-NPC switching orders, low consideration for the switching frequency

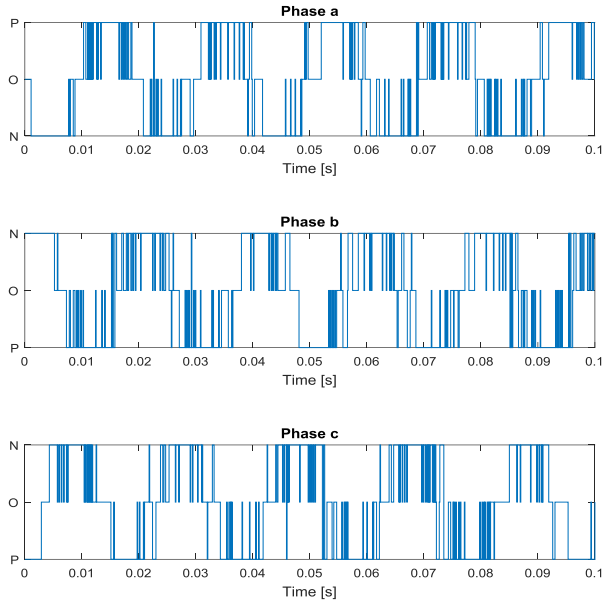

Fig. 9: 3L-NPC switching orders, high consideration for the switching frequency

From the scheme in Fig. 1(b), the converter possesses four different binding positions by phase. The precedent notation is adapted in Table 3 and leads to the equation set (15) to (18).

$$\frac{CdU_{-c1}}{dt} = \sum_{x=a,b,c}(S_{x1} + S_{x0+}) \tag{15}$$

$$C\frac{dU_{-c2}}{dt} = \sum_{x=a,b,c} -(S_{x2} + S_{x0-})i_x - i_{DC} \tag{16}$$

$$C\frac{dU_{cx}}{dt} = (S_{x0+} - S_{x0-})i_x - i_{DC}\ ; x = a,b,c \tag{17}$$

$$V_{gx} - V_0 = R_g i_x + L_g\frac{di_x}{dt} + (S_{x1} + S_{x0+})U_{c1} + (S_{a0+} - S_{a0-})U_{cx} - (S_{x2} + S_{x0-})U_{c2}\ ; x = a,b,c \tag{18}$$

The matrices $\mathbf{A_{conv\_1}}$, $\mathbf{A_{conv\_2}}$ and $\mathbf{B}$ are described in (19), (20) and (21), with $\mathbf{x}^{\mathrm{T}}=[i_a\ i_b\ i_c\ U_{ca}\ U_{cb}\ U_{cc}\ U_{c1}\ U_{c2}]$ and $\mathbf{d}^{\mathrm{T}} = [V_{ga}\ V_{gb}\ V_{gc}\ i_{DC}]$.

$$\mathbf{A_{conv\_1}} = \frac{1}{L_g}\begin{pmatrix} S_{a0+} - S_{a0-} & 0 & 0 & S_{a1} + S_{a0+} & -S_{a2} + S_{a0-} \\ 0 & S_{b0+} - S_{b0-} & 0 & S_{b1} + S_{b0+} & -S_{b2} + S_{b0-} \\ 0 & 0 & S_{c0+} - S_{c0-} & S_{c1} + S_{c0+} & -S_{c2} + S_{c0-} \end{pmatrix} \tag{19}$$

$$\mathbf{A_{conv\_2}} = \frac{1}{C}\begin{pmatrix} S_{a0+} - S_{a0-} & 0 & 0 & 0 & 0 \\ 0 & S_{b0+} - S_{b0-} & 0 & 0 & 0 \\ 0 & 0 & S_{c0+} - S_{c0-} & 0 & 0 \\ -S_{a1} + S_{a0+} & -S_{b1} + S_{b0+} & -S_{c1} + S_{c0+} & 0 & 0 \\ S_{a2} + S_{a0-} & S_{b2} + S_{b0-} & S_{c2} + S_{c0-} & 0 & 0 \end{pmatrix} \tag{20}$$

$$\mathbf{B} = \left(\frac{1}{L_g C}\begin{bmatrix} \mathbf{I_3}C & \mathbf{O_{3,1}} \\ \mathbf{O_{1,3}} & -L_g \\ \mathbf{O_{1,3}} & L_g \end{bmatrix}\right) \tag{21}$$

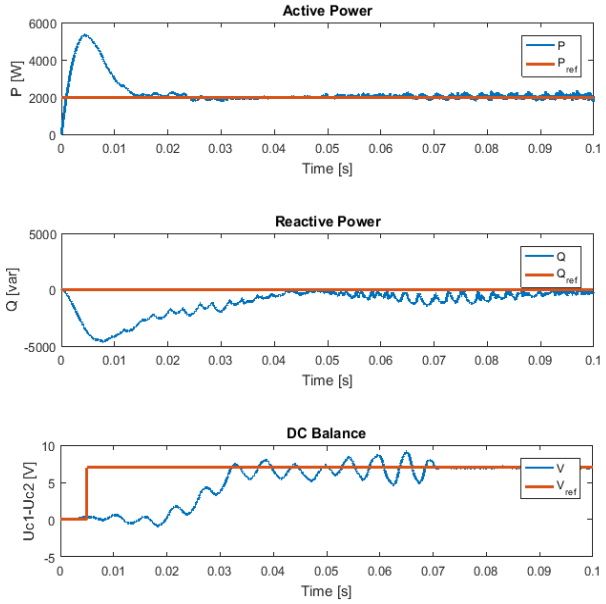

Fig. 11: 3L-FC tracking

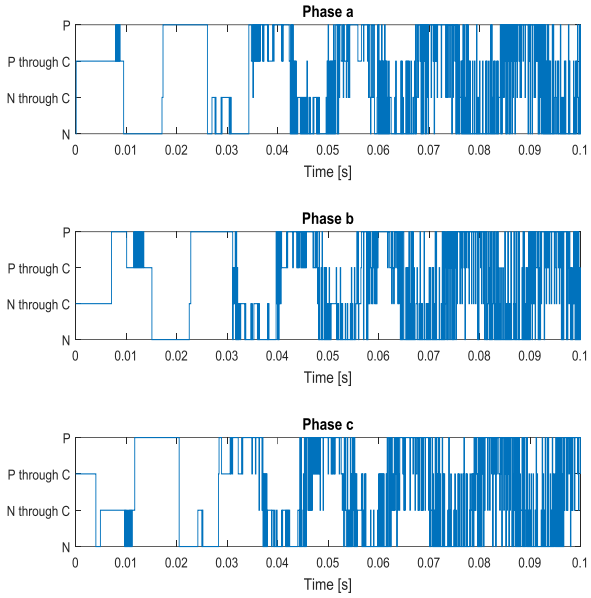

Fig. 12: 3L-FC switching orders

The proposed controller is able to manage every degrees of freedom of the converter, as shown in Fig. 11. The same processor used previously required a mean time of 50 µs. Similar to the precedent case, fostering the number of commutations entails a deterioration of the tracking performance but does not prevent the goal achievement. A trade-off between tracking performances should be found when the control strategy is designed.

V. Conclusion

In this paper a generic methodology to design a MPC controller for multi-level converters was presented. This method is feasible and can be extended to any application and topology, without modulation. It does not need any restrictive hypothesis on the system and can manage a large variety of requirements. Simulations are being run to prove the abilities of the proposed direct-state-space technique, and results show the capacity of the controller to carry out complex power management tasks under reliability conditions.

References:

[1] F. Blaabjerg and K. Ma, "Future on Power Electronics for Wind Turbine Systems," IEEE Journal of Emerging and Selected Topics in Power Electronics, vol. 1, no. 3, pp. 139–152, Sep. 2013.

[2] H. Wang, M. Liserre and F. Blaabjerg, "Toward reliable power electronics: Challenges, design tools, and opportunities," IEEE Industrial Electronics Magazine, vol. 7, no. 2, pp. 17–26, Jun. 2013.

[3] S. Vazquez, J. Rodriguez, M. Rivera, L. G. Franquelo, and M. Norambuena, "Model predictive control for power converters and drives: Advances and trends," IEEE Transactions on Industrial Electronics, vol. 64, no. 2, pp. 935–947, Feb. 2017.

[4] A. Susperregui, M. I. Martinez, G. Tapia, and I. Vechiu, "Second-order sliding-mode controller design and tuning for grid synchronisation and power control of a wind turbine-driven doubly fed induction generator," IET Renewable Power Generation, vol. 7, no. 5, pp. 540–551, Sep. 2013.

[5] M. I. Martinez, A. Susperregui, and G. Tapia, "Second-order sliding-mode-based global control scheme for wind turbine-driven DFIGs subject to unbaslanced and distorted grid voltage," IET Electric Power Applications, vol. 11, no. 6, pp. 1013–1022, Jul. 2017.

[6] E. Camacho and C. Bordons, Model Predictive Control. Springer Science&Business Media, 2013.

[7] Q. Tabart, I. Vechiu, A. Etxeberria, S. Bacha, " Hybrid energy storage system microgrids integration for power quality improvement using fur leg three level NPC invertir and second-order sliding mode control," IEEE Transactions on Industrial Electronics , DOI: 10.1109/TIE.2017.2723863.

[8] J. Rodriguez and P. Cortes, "Predictive control of a three-phase neutral-point clamped inverter," Predictive Control of Power Converters and Electrical Drives, 1, Wiley-IEEE Press, 2012, pp. 65–79.

[9] J. A. Bondy, Graph Theory with Applications. Elsevier Science Ltd, 1976.

[10] E. Dijsktra, A Short Introduction to the Art of Programming. Techn. Hogeschool, 1971.

[11] A. Nabae, I. Takahashi and H. Akagi, "A new neutral point clamped PWM inverter" IEEE Transaction on Industrial Applications, vol. IA-17, no. 5, pp. 518–522, Sep.-Oct. 1981.

[12] T. A. Meynard, H. Foch, P. Thomas, J. Courault, R. Jakob, and M. Nahrstaedt "Multi-cell converters: Basic concepts and industry applications," IEEE Transactions on Industrial Electronics, vol. 49, no. 5, pp. 955–964, Oct. 2002.